

# PROCEEDINGS OF SPIE

[SPIEDigitallibrary.org/conference-proceedings-of-spie](https://www.spiedigitallibrary.org/conference-proceedings-of-spie)

## On-machine metrology for diamond turning applications

Wenjun Kang, Yihan Wang, Hongzhang Ma, Daodang Wang, Rongguang Liang

Wenjun Kang, Yihan Wang, Hongzhang Ma, Daodang Wang, Rongguang Liang, "On-machine metrology for diamond turning applications," Proc. SPIE 12672, Applied Optical Metrology V, 1267208 (4 October 2023); doi: 10.1117/12.2677505

**SPIE.**

Event: SPIE Optical Engineering + Applications, 2023, San Diego, California, United States

# On-machine metrology for diamond turning applications

Wenjun Kang<sup>a</sup>, Yihan Wang<sup>a</sup>, Hongzhang Ma<sup>a</sup>, Daodang Wang<sup>†a</sup>, Rongguang liang<sup>‡a</sup>,

<sup>a</sup>Wyant College of Optical Science, The University of Arizona, Tucson, AZ, 85719, USA

## ABSTRACT

A dual-mode on-machine metrology system has been developed to address the critical demand for on-machine metrology in precision optics fabrication. The system can measure both surface form and roughness simultaneously, without requiring the reconfiguration of the optical path to switch between laser interferometer mode and LED interference microscopy mode. It can achieve snapshot high-precision phase-shifting measurement, minimizing the impact of environmental disturbance. With its compact design, the system makes on-machine metrology feasible in diamond turning machines, avoiding errors caused by removing, repositioning, and balancing the workpiece. With the compact and dual-mode features, it makes on-machine tool alignment and surface characterization possible, avoiding off-line testing and significantly increasing process efficiency.

**Keywords:** On-machine metrology, interferometer, dual-mode, diamond turning

## 1. INTRODUCTION

High-quality surface finishes are increasingly demanded across modern industries, particular for the functional optical surfaces used in optics, machinery manufacturing, biomedicine, national defense, and the military [1, 2]. The current major precision fabrication technologies for optics include grinding, polishing, 3D printing, lithography, and diamond turning [3-6]. Among these methods, ultra-precision single point diamond turning (SPDT) stands out as commercially viable and easily scalable. The trend of increasing miniaturization and automation of optical applications drives the need for more stringent tolerance and surface finish requirements [7]. While quality control poses challenges in optical fabrication, such as the need for precision surface shape and roughness measurements, the use of feedback control is vital to ensure production conformance. Through compensation machining using surface measurement data, the accuracy can be enhanced in ultra-precision SPDT, thus further expanding its fabrication capabilities [8]. Conventional post-process quality inspection is usually carried out offline using commercial measurement tools, which involves unclamping and re-mounting specimens, and it can introduce errors, disrupt workflow, and limit production rates. To address these issues, on-machine metrology (OMM) offers a viable solution by performing measurements directly within the machine tool environment, facilitating precision SPDT tool alignment.

OMM can be divided into two types: tactile and optical systems [9]. In contact OMM applications, sapphire and diamond microprobes equipped with precision displacement sensors like linear variable differential transformer (LVDT) have been utilized for various applications, such as: compensate profile errors in grinding tungsten carbide molds, assist measuring in a desktop ultra-precision machine, and carrying out freeform areal surface scanning [10-12]. To decouple surface profiles from SPDT slide axis errors in the probe based OMM measurement process, a reversal technique was proposed to address this issue [13]. However, contact probe measurements can alter surface topology fidelity by applying probe-tip-size mechanical spatial filter. Moreover, applying constant force across different materials with varying hardness and surface topography can result in data validity issues. Worst of all, this approach can potentially lead to surface scratches and damage on the workpiece surface. Optical metrology systems are known for their non-contact nature, and in terms of OMM setup, chromatic confocal technology is commonly reported. By evaluating uncertainty in on-machine chromatic confocal measurement on a micro-electrical discharge machining, the significant uncertainty contributions from vibration disturbances and machine axis drive unit can be identified [14]. To achieve optimal performance, the studies on scanning path strategies and careful alignment [15] are crucial. Through point-by-point scanning acquisition, a similar confocal probe is adopted for OMM to study the form error introduced by SPDT  $X$ -axis deviation and the tool alignment [16]. However, scanning confocal probe based OMM still faces challenges, including high sensitivity to environmental

---

<sup>†</sup> email: [wangdaodang@arizona.edu](mailto:wangdaodang@arizona.edu);

<sup>‡</sup> email: [rliang@optics.arizona.edu](mailto:rliang@optics.arizona.edu)

disturbance, long scanning time, low spatial resolution, position error, and intensive post-data processing which involves fitting and filtering [17].

To overcome the drawbacks of point-by-point acquisition, various fast full-aperture measurement methods have been developed, including hybrid vision systems, deflectometry, and interferometry [18-21]. Among these methods, interferometry-based full-aperture measurement is highly accurate and commonly used for characterizing high-quality optical surfaces. However, most interferometric systems are designed as off-machine and single-working-mode devices, such as conventional phase-shifting interferometry (PSI) and white light interferometry (WLI), which are designed to measure either surface shape or roughness, but not both. Additionally, PSI is affected by ambient vibration during phase stepping intensity acquisition process, requiring further data processing to mitigate the impact [22]. To overcome these limitations, a compact and rapid measurement system that is accurate and less sensitive to environmental disturbance is needed. The pixelated phase-mask interferometer has been developed [23-27].

To address the critical demand for OMM in precision optics fabrication, we have developed a dual-mode OMM system to realize both the surface form and roughness measurements, including laser interferometer mode and LED interference microscopy mode. It doesn't require the reconfiguration of the optical path to switch between the working modes, and the compact configuration also provides feasibility of integration inside SPDT machines. Its snapshot feature avoids long phase-shifting acquisition time and minimizes external environmental impact. With the OMM and dual-mode features, it enables on-machine surface characterization and tool alignment. In this paper, we explore its different fabrication applications with on-machine measurement implementation to give rapid feedback. The results are also compared with the ones acquired by Zygo WLI and Fizeau PSI to prove the effectiveness of the proposed OMM system.

## 2. SYSTEM CONFIGURATION AND PRINCIPLES

The configuration setup of the proposed dual-mode interferometric OMM system is shown in Figure 1, which can work in both laser interferometer mode and LED interference microscopy mode. In LED interference microscopy mode, an LED with central wavelength 530 nm and bandwidth 10 nm serves as a light source. The LED beam goes through a folded dichroic mirror (DM - short pass, transmit LED light, reflect Laser light) and then a linear polarizer (LP). The LP is used to adjust the relative light intensities between test and reference arms, by which the adjustable interference fringe contrast can be achieved. After passing the beam splitter (BS) and polarizing beam splitter (PBS), the linearly polarized light is divided into two parts: p-polarized light and s-polarized light. The p-polarized light passes through the PBS and an optical-path-matching window (OP-W), objective, tested surface, and then goes back along the same path, serving as test beam; while the s-polarized light is reflected by the PBS, then transmitted through a short-pass optical filter (OF - transmit LED light, reflect Laser light), objective, eventually reaching reference mirror (RM) and goes back along the same path, serving as reference beam. Both the test and reference beams combine at PBS and then are reflected by BS. After transmitting through a quarter-wave plate (QWP) with fast axis oriented at 45-degree to horizontal direction, the linearly polarized reference and test beams are transformed into being oppositely circularly polarized, and then imaged on a pixelated polarization camera (P-CAM) by an imaging lens. The P-CAM has four linear polarizers at 0°, 45°, 90° and 135° built inside, forming a 2×2 superpixel. The P-CAM enables the snapshot phase shifting measurement by capturing four phase-shifted interferograms without motion.

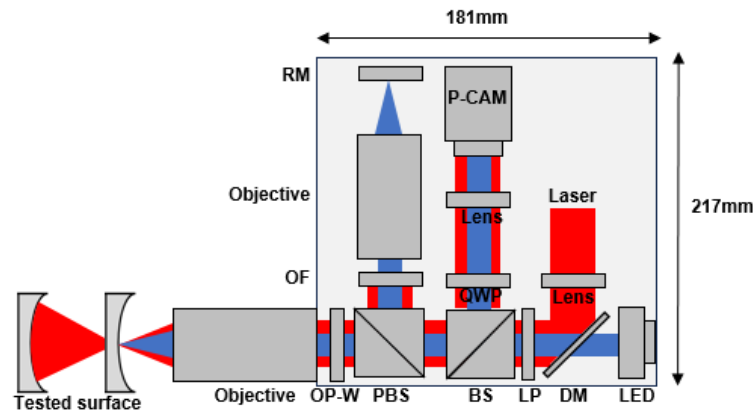


Figure 1. System layout of the proposed OMM system.

While in laser interferometer mode, the system uses a 632.8 nm laser as light source. The collimated laser beam is reflected by the DM, then entering the common path configuration shared with LED interference microscopy mode. Different from the LED interference microscopy mode, the s-polarized light at reference arm is reflected by OF, rather than the reference mirror RM. With this common-path configuration, the system has a compact dimension of 181 mm × 217 mm. Switching measurement modes is easily accomplished by toggling the ON/OFF state of the two different light sources.

With the four stepped-phase interferograms acquired by P-CAM in a single shot, which can be denoted as  $I_0(x, y)$ ,  $I_{45}(x, y)$ ,  $I_{90}(x, y)$ ,  $I_{135}(x, y)$ , the phase information  $\varphi(x, y)$  and the corresponding testing surface topography  $Height(x, y)$  can be obtained as

$$\varphi(x, y) = \tan^{-1} \left( \frac{I_{135}(x, y) - I_{45}(x, y)}{I_0(x, y) - I_{90}(x, y)} \right), \quad (1)$$

$$Height(x, y) = \frac{\lambda}{4\pi} \varphi(x, y), \quad (2)$$

where  $\lambda$  is the beam wavelength.

### 3. OMM APPLICATIONS

To verify the performance and effectiveness of the proposed OMM system, the experiments were carried out on a Nanotech 350FG machine, as illustrated in Figure 2. Both high-reflectivity brass stud and low-reflectivity polymethyl methacrylate (PMMA) have been tested. As comparison results, commercial offline Zygo NewView 8300 WLI and Fizeau PSI measurements were also performed. The objective of OMM has NA of 0.42, and Zygo WLI has NA of 0.4.

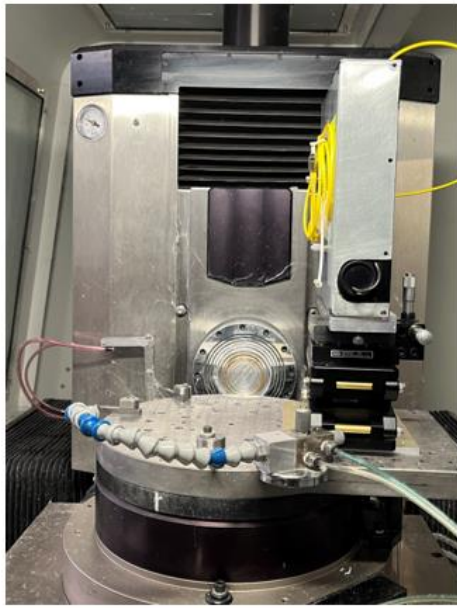


Figure 2. OMM setup on Nanotech 350FG machine for on-machine measurement.

#### 3.1 High-reflectivity material measurement

The high-reflectivity surface to be measured is a brass surface. Figure 3(a) shows a center region of diamond turned ogive surface measurement result captured by OMM, with the surface root mean square (RMS) value of 5.95 nm. With same testing surface measured by offline Zygo NewView 8300 WLI, the comparable result is shown in Figure 3(b), and the surface RMS value is 6.00 nm. Both the measurements can detect the center pit clearly, and the 11.6  $\mu\text{m}$  offset of diamond tool in Y-axis can be inferred. Utilizing the tool offset shift from the OMM result as the retooling feedback during tool alignment process, the corresponding measurement results captured by OMM and offline WLI after retooling are given in Figures 3(c) and 3(d). It can be seen from Figures 3(c) and 3(d), the measurement results from the two systems are identical, and the center pit has been removed after retooling.

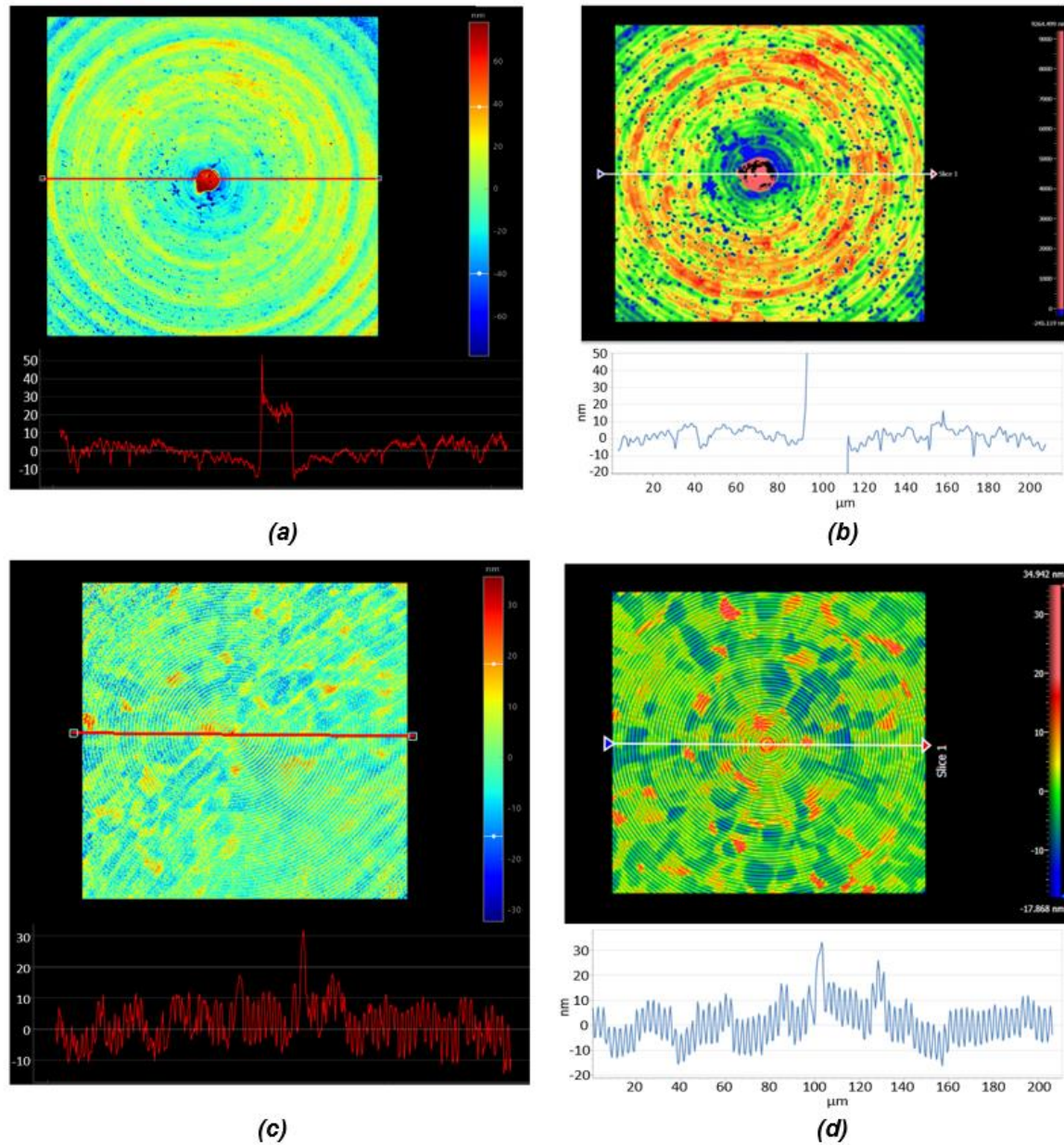


Figure 3. Surface roughness measurement results corresponding to Y-shifted tool induced diamond turning result of brass. (a) and (b) surface roughness measurement results are from the proposed OMM and commercial Zygo NewView 8300 WLI corresponding to Y-shifted tool induced diamond turning result of brass. (c) and (d) surface roughness measurement results are from the proposed OMM and commercial Zygo NewView 8300 WLI after OMM result feedback.

Similarly, to determine the diamond tool offset in X axis, the ogive surface has been measured with OMM and the acquired result is shown in Figure 4(a), from which the peak-to-valley (PV) value around 500 nm is observed. It is confirmed with result (Figure 4(b)) measured with Zygo Fizeau PSI. According to the surface measurement result, the X offset can be calculated and provided as a feedback for retooling directly. To verify the offset correction effectiveness, the retooled surface is measured again by OMM, with the result being shown in Figure 4(c), and the PV dropped down to 60 nm. For comparison, Zygo Fizeau measurement result of the retooled surface is also acquired, as is shown in Figure 4(d). According to Figure 4(d), the slice profiles across the center is identical to that from OMM, by which the effectiveness of OMM utilization in tool alignment process can be proved.

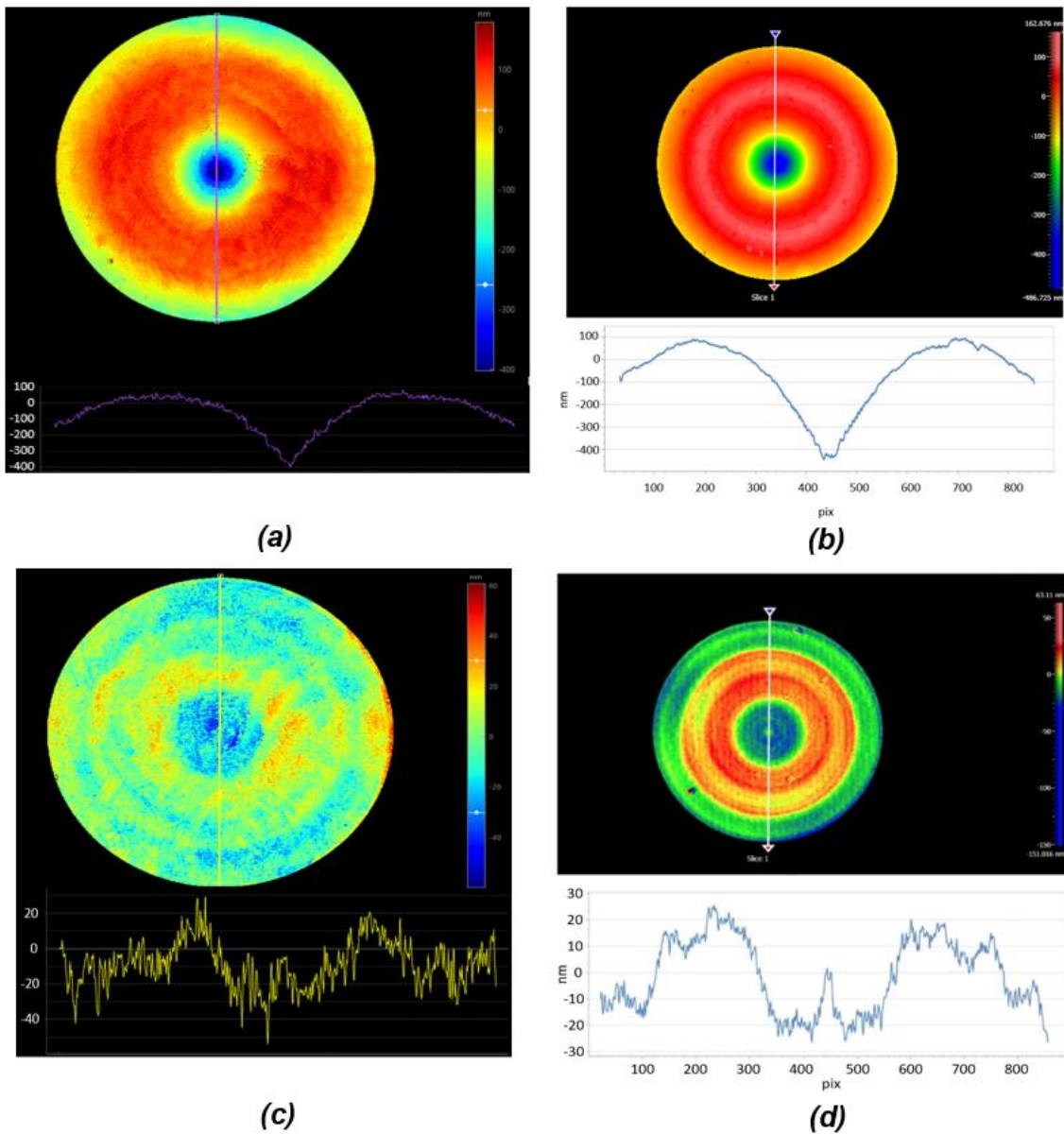


Figure 4. Surface form measurement results corresponding to diamond turning ogive surface of brass with X offset. (a) and (b) surface form measurement results of the ogive surface are from the proposed OMM and commercial Zygo Fizeau PSI. (c) and (d) retooled surface form measurement results are from the proposed OMM and commercial Zygo Fizeau PSI after retooling with the feedback of OMM measurement result.

### 3.2 Low-reflectivity material measurement

To further demonstrate the flexibility of the proposed OMM system, the PMMA surface with low reflectivity of around 4% was tested. For conventional commercial PSI, switching from high-reflectivity material to low-reflectivity material, the testing configuration needs to be modified either by removing attenuator or changing to another low-reflectivity reference to increase fringe visibility for alignment and sensor detection. While our OMM simplified the process and reduced the cost by simply rotating the linear polarizer. The PMMA surface roughness measurement result acquired by the proposed OMM is shown in Figure 5. According to Figure 5, the unique diamond tool finished cusp structure is clearly observed, and the PV value of local tool mark is around 100 nm which is finished with a small radius of diamond tool.

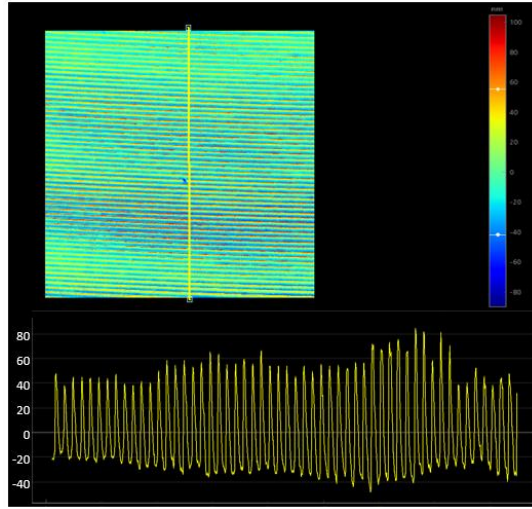


Figure 5. Surface roughness measurement result of diamond turned PMMA surface acquired by OMM.

In addition, the measurement of a flat PMMA surface form has also been performed with OMM. Figure 6 gives the OMM measurement result for PMMA surface form, with the PV value of cross-section slice profile being below 60 nm.

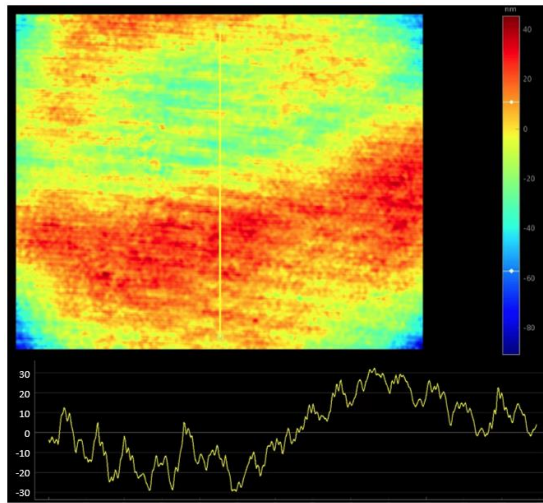


Figure 6. Surface form measurement result of diamond turned PMMA surface acquired by OMM.

#### 4. CONCLUSION

In this paper, an OMM system for multiple diamond turning applications is proposed to meet the demand for on-machine metrology in precision optics fabrication. The system presents unique advantages of compact size and snapshot measurement, enabling easy integration within diamond turning machine. By performing the on-machine surface roughness and form testing of the high-reflectivity brass material and low-reflectivity PMMA material, the flexibility and effectiveness of the proposed OMM system has been validated. Furthermore, the dual working modes make it applicable for on-machine diamond tool alignment and rapid measurement feedback, avoiding off-line testing and significantly increasing process efficiency.

#### ACKNOWLEDGEMENTS

This work is supported by National Science Foundation (1918260).

## REFERENCES

- [1] Rolland, J. P., Davies, M. A., Suleski, T. J., Evans, C., Bauer, A., Lambropoulos, J. C., and Falaggis, K., "Freeform optics for imaging," *Optica* 8(2), 161-176 (2021).
- [2] Yin, S., Xiao, H., Kang, W., Wu, H., and Liang, R. "Shoulder damage model and its application for single point diamond machining of ZnSe crystal." *Materials*, 15(1), 233(2021).
- [3] Komanduri, R., Lucca, D. A., and Tani, Y., "Technological advances in fine abrasive processes." *CIRP annals*, 46(2), 545-596(1997).
- [4] Kang, W., Hong, Z., and Liang, R., "3D printing optics with hybrid material." *Applied Optics* 60(7), 1809-1813 (2021).
- [5] Fang, F. Z., Zhang, X. D., Weckenmann, A., Zhang, G. X., and Evans, C., "Manufacturing and measurement of freeform optics," *CIRP Annals* 62(2), 823-846 (2013).
- [6] Kang, W., Seigo, M., Xiao, H., Wang, D., and Liang, R., "Experimental Studies on Fabricating Lenslet Array with Slow Tool Servo." *Micromachines*, 13(10), 1564(2022).
- [7] G. Tosello, H.N. Hansen, S. Gasparin, "Applications of dimensional micro metrology to the product and process quality control in manufacturing of precision polymer micro components," *CIRP Annals* 58(1), 467-472 (2009)
- [8] Gao, W., Tano, M., Araki, T., Kiyono, S., and Park, C. H., "Measurement and compensation of error motions of a diamond turning machine," *Precision Engineering* 31(3), 310-316 (2007).
- [9] Gao, W., Haitjema, H., Fang, F. Z., Leach, R. K., Cheung, C. F., Savio, E., and Linares, J. M., "On-machine and in-process surface metrology for precision manufacturing," *CIRP Annals* 68(2), 843-866 (2019).
- [10] Chen, F. J., Yin, S. H., Huang, H., Ohmori, H., Wang, Y., Fan, Y. F., and Zhu, Y. J., "Profile error compensation in ultra-precision grinding of aspheric surfaces with on-machine measurement," *International Journal of Machine Tools and Manufacture* 50(5), 480-486 (2010).
- [11] Liu, Y. T., Kuo, Y. L., and Yan, D. W., "System integration for on-machine measurement using a capacitive LVDT-like contact sensor," *Advances in Manufacturing* 5(1), 50-58 (2017).
- [12] Davies, M. A., Dutterer, B. S., Swagler, S., Lawing, E., Horvath, N., Rolland, J. P., and Bauer, A., "Optomechanical design and fabrication of a wide field of view 250-mm-aperture freeform imaging system," in *Proc. 22nd Advanced Maui Optical and Space Surveillance Technologies (AMOS) Conf.* (Maui, HI) (2021).
- [13] Gao, W., Shibuya, A., Yoshikawa, Y., Kiyono, S., and Park, C. H., "Separation of scanning error motions for surface profile measurement of aspheric micro lens," *International Journal of Manufacturing Research* 1(3), 267-282 (2006).
- [14] Ye, L., Qian, J., Haitjema, H., and Reynaerts, D., "Uncertainty evaluation of an on-machine chromatic confocal measurement system." *Measurement* 216, 112995 (2023).
- [15] Shibuya, A., Arai, Y., Yoshikawa, Y., Gao, W., Nagaike, Y., and Nakamura, Y., "A spiral scanning probe system for micro-aspheric surface profile measurement," *The International Journal of Advanced Manufacturing Technology* 46, 845-862 (2010).
- [16] Chen, Z., Wang, Z., Ren, M., Zhang, X., Zhu, L., and Jiang, X., "Development of an on-machine measurement system for ultra-precision machine tools using a chromatic confocal sensor," *Precision Engineering* 74, 232-241 (2022).
- [17] Nadim, E. H., Hichem, N., Nabil, A., Mohamed, D., and Olivier, G., "Comparison of tactile and chromatic confocal measurements of aspherical lenses for form metrology," *International Journal of Precision Engineering and Manufacturing* 15, 821-829 (2014).
- [18] Teti, R., Mourtzis, D., D'Addona, D. M., and Caggiano, A., "Process monitoring of machining." *CIRP Annals* 71(2), 529-552 (2022).
- [19] Zhu, S., Wang, D., Kang, W., and Liang, R., "On-axis deflectometric system for freeform surface measurement," *Optics Letters* 48(8), 1986-1989 (2023).
- [20] Jiang, X., "In situ real-time measurement for micro-structured surfaces," *CIRP Annals* 60(1), 563-566 (2011).
- [21] Yan, J., Baba, H., Kunieda, Y., Yoshihara, N., and Kuriyagawa, T., "Nano precision on-machine profiling of curved diamond cutting tools using a white-light interferometer," *International Journal of Surface Science and Engineering* 1(4), 441-455 (2007).
- [22] Deck, L. L., "Model-based phase shifting interferometry," *Applied Optics* 53(21), 4628-4636 (2014).
- [23] Millerd, J., Brock, N., Hayes, J., North-Morris, M., Kimbrough, B., and Wyant, J., "Pixelated phase-mask dynamic interferometers," in *Fringe 2005: The 5th International Workshop on Automatic Processing of Fringe Patterns* (pp. 640-647). Springer Berlin Heidelberg (2006).
- [24] Wyant, J. C., "Computerized interferometric measurement of surface microstructure," *Proc. SPIE* 2576, 122-130 (1995).

- [25] Wang, D., and Liang, R., "Simultaneous polarization Mirau interferometer based on pixelated polarization camera," *Optics Letters* 41(1), 41-44 (2016).
- [26] Wang, D., Tian, X., Xu, P., Liang, J., Wu, H., Spires, O., and Liang, R., "Compact snapshot multiwavelength interferometer." *Optics Letters*, 44(18), 4463-4466(2019).
- [27] Wang, D., Fu, X., Xu, P., Tian, X., Spires, O., Liang, J., Wu H., and Liang, R. "Compact snapshot dual-mode interferometric system for on-machine measurement. " *Optics and Lasers in Engineering*, 132, 106129(2020)